Journal of Air Pollution and Health (Winter 2026); 11(1): 77-94

Original Article

Available online at http://japh.tums.ac.ir

Computational fluid dynamics (CFD) simulation of airborne toxic pollutants and associated human health risks in industrial zones of Delta state, Nigeria

Nkechi Blessing Chinedu[1], Gospel Effiong Isangadighi[2,*], Ubong Bernard Essien[3], Salami Basirat Adedamola[4], Austin Uzochukwu Orabuego[5], Patience Oinu Momoh[6]

[1] Department of Industrial Chemistry, Southern Delta University, Delta State, Nigeria
[2] Environmental Management and Toxicology, Federal University of Petroleum Resources, Effurun, Delta State, Nigeria
[3] African Centre of Excellence in Public Health and Toxicological Research, University of Port Harcourt, Rivers State, Nigeria
[4] Department of Chemical Sciences, Lead City University, Oyo State, Nigeria
[5] Pharmacology and Toxicology, Pharmaceutical Sciences University of Nigeria, Nsukka, Nigeria
[6] Department of Public Health, Global Health and Infectious Disease Control Institute (GHIDI), Nasarawa State University, Keffi, Nasarawa State, Nigeria

ARTICLE INFORMATION

Article Chronology:
Received 19 October 2025
Revised 05 January 2026
Accepted 15 February 2026
Published 29 March 2026

Keywords:
Computational fluid dynamics (CFD); Airborne toxic pollutants; Human health risk assessment (HHRA); Industrial emissions; Delta state, Nigeria

CORRESPONDING AUTHOR:
isangadighigospelpgschool@fupre.edu.ng
Tel: 2349078830838
Fax: 2349078830838

ABSTRACT

Introduction: The rapid rate of industrial growth in Delta State, Nigeria, has led to an increase in the emission of airborne pollutants, including Particulate Matter ($PM_{2.5}$), Sulfur dioxide (SO_2), Nitrogen Oxides (NOx), and Volatile Organic Compounds (VOCs), which pose a threat to the environment and the health of the population. This paper utilises Computational Fluid Dynamics (CFD) and Human Health Risk Assessment (HHRA) to simulate the dispersion of pollutants and assess the risks associated with exposure in four industrial areas: Warri/Ekpan, Aladja, Ughelli, and Kwale.

Materials and methods: Simulations in three-dimensional CFD of ANSYS Fluent 2024 R1 were conducted using the actual meteorological, topographic and emission parameters provided in NiMet and EIA data. The Navier-Stokes equations were solved with the Realisable k-epsilon turbulence model. The model results were georeferenced and interpreted in ArcGIS Pro 3.2, generating exposure maps by combining the pollutant fields with the population fields. The Hazard Index (HI) and Lifetime Cancer Risk (LCR) were used in quantifying health risks in accordance with USEPA guidelines.

Results: The concentrations of VOCs and $PM_{2.5}$ in the air were 115.6 µg/m³ and 56.2 µg/m³, respectively, which exceeded the WHO levels. HI values were 14.7-21.4 (adults) and 26.138.0 (children), and LCR values (1.710;-3.210; -3) represented that there was carcinogenic risk.

Conclusion: CFDH-HRA was the most accurate in predicting risks of pollution and exposure, highlighting hotspots in critical zones near Warri and Aladja. The importance of adopting CFD-based control and monitoring to achieve SDGs 3, 9, 11, and 13 lies in creating a cleaner and healthier environment.

Please cite this article as: Chinedu NB, Isangadighi GE, Essien UB, Adedamola SB, Orabuego AU, Momoh PO. Computational fluid dynamics (CFD) simulation of airborne toxic pollutants and associated human health risks in industrial zones of Delta state, Nigeria. Journal of Air Pollution and Health. 2026;11(1): 77-94.
Doi: https://doi.org/10.18502/japh.v11i1.21271

Introduction

Air pollution has been one of the most pressing environmental and health issues worldwide, particularly in the industrial and urban areas of developing countries. All these decontamination of oil, flaring of gas, manufacture of steel and petrochemicals release intricate blends of airborne toxic emissions comprising Volatile Organic Compounds (VOCs), Sulphur dioxide (SO_2), Nitrogen Oxides (NOx) and Particulate Matter ($PM_{2.5}$ and PM_{10}), which are major contributors to the poor quality of air in the atmosphere [1-3]. These sulphuric materials are closely linked with respiratory conditions, cardiac issues, malignancies, and early death with use of the substances [4]. The diffusion and retention of such pollutants in the atmosphere are regulated by meteorological processes, which include the speed and direction of wind, temperature, humidity, and terrain and built-environment characteristics [5]. It is only through these dispersion patterns that human health can be secured and a certain level of sustainability in industrial development attained. Finally, Delta State is a Tier-1 city in Nigeria, situated in the oil-rich Niger Delta region, where large industrial plants, including refineries, petrochemical plants, and steel production facilities, are located [6, 7]. These properties emit large volumes of gaseous and particulate pollutants into the atmosphere, resulting in poor air quality in this area and health risks to the residents. SO_2, NO_2, and hydrocarbons have been reported to be at very high levels in the ambient air of industrial towns, such as Warri, Aladja, Ughelli, and Ekpan, exceeding national and World Health Organisation (WHO) standards [8]. Most works in the area have, unfortunately, been based on either ground-based observations or empirical investigations, which lack spatial and temporal resolution and thus do not capture the intricate dynamics of pollutant dispersion under different meteorological conditions. This restriction calls for superior modelling methods that can represent the airflow and transport of pollutants in industry more realistically.

Computer-aided fluid dynamics (1) CFDF has been a potent tool to model the behaviour of air pollutants within the atmospheric boundary layer. CDF allows for visualising the dispersal and turbulence of pollutants and their concentration gradients at a three-dimensional level through a numerical solution of the species' convection equation and the equation of motion, namely the Navier-Stokes equations [9, 10]. Unlike typical Gaussian models, the CFD is highly complex in terms of the detail of its description of pollutant transport because it is capable of capturing the local impact of terrain, the character of buildings, and short-period weather conditions. Combining the concept of Human Health Risk Assessment (HHRA) developed by the United States Environmental Protection Agency [11], CFD simulations can be used to identify potential non-carcinogenic and carcinogenic risks of exposure to contaminants. The researchers were able to compare the simulated levels of pollutants with human health through the following parameters: Hazard Quotient (HQ), Hazard Index (HI) and Lifetime Cancer Risk (LCR) [12, 13]. Although CFDs have been established as applicable, there is still a lack of air quality and health risk modelling of CFDs in Nigeria, particularly in Delta State, where emissions are particularly high. The current literature has primarily focused on monitoring the environment or chemical traits, without examining the trends in spatial distribution and the dynamics of population exposure [7]. The research gap is essential in addressing the commitment by the United Nations to the Sustainable Development Goals (SDGs) through implementing SDG 3 (Good Health and Well-being), SDG 6 (Clean Water and Sanitation), SDG 9 (Industry, Innovation, and Infrastructures), SDG 11

(Sustainable Cities and Communities) and SDG 13 (Climate Action) in Nigeria. The findings of this study will enable the provision of an innovative, evidence-based model to examine the environment and the impacts of industrial air pollution on the health of people in Delta State. This will be achieved by integrating CFD simulation with human health risk assessment. Lastly, the proposed study outcomes would aid in making data-driven decisions, promoting sustainable industrial regulation, and enhancing health rates among the population in industrial areas in Nigeria.

Materials and methods

Study area description

The study was conducted in major industrial regions of Delta State, Nigeria: Warri/Ekpan, Aladja, Ughelli, and Kwale, which are the primary centres of Industries and petrochemical operations within the state. They were selected because they have large-scale operations such as the Warri Refining and Petrochemical Company (WRPC), Delta Steel Company (DSC) at Aladja, gas processing plants of Ughelli and Kwale, which are the significant sources of Volatile Organic Compounds (VOCs), Sulphur dioxide (SO_2), Nitrogen Oxides (NOx) and $PM_{2.5}$ and PM_{10}. Delta state is located between latitudes 5° and 6°30' N, and longitudes 50° and 64°50' E, with a high level of humidity (more than 80%) and temperatures ranging between 27° and 30 °C. The southwest wind facilitates the transport of pollutants from industrial clusters to the surrounding settlements.

Meteorological and emission input data

Meteorological data, including wind direction, temperature, and speed, along with land elevation and terrain data, were obtained from the Nigerian Meteorological Agency (NiMet), the Shuttle Radar Topography Mission (SRTM), and the Nigerian Geological Survey Agency (NGSA). The parameters of emissions, including the stack height, gas velocity, and pollutant release rates, were obtained based on the Environmental Impact Assessment (EIA) reports and literature on analogous industrial systems.

FD modelling framework

The simulations using the Computational Fluid Dynamics (CFD) model were conducted in ANSYS Fluent 2024 R1, employing a three-dimensional model of approximately 2 km x 2 km x 0.5 km to represent each industrial space. The realisable k-epsilon turbulence model was used to solve the Navier-Stokes equations (RANS) in the form of turbulent averages, effectively revealing near-ground atmospheric turbulence. Boundary conditions were set for the Inlet boundary, which follows a logarithmic wind velocity profile based on field data; the outlet, with a pressure outlet condition; the wall roughness element; and the no-slip wall element of the ground and buildings. The top boundary was considered a plane of symmetry. Stacks added pollutant emissions as point sources, and steady-state and transient simulations were used to reflect both the average and episodic releases under dry-season meteorological conditions. More grid resolution was optimised, and the most significant numerical diffusion was minimised through mesh independence tests. The model validation was based on the comparison of simulated concentrations with published field data at Delta State.

CFD output export and georeferencing

The three-dimensional concentration fields simulated in ANSYS Fluent 2024 R1 were saved as Power Georges (.csv) and triangulated (.vtk) files to analyse individual geospatial data on the triangular formations thoroughly. The steady-state outcomes estimated at an altitude of 1.5 m above the ground (breathing height) were used

over time. There was a spacing of 10 m between receptor grids, resulting in high-resolution 2D fields of polar concentrations. The coordinates of the CFD models were georeferenced with respect to the latitude and longitude provided in the known stack of industrial stacks, which were obtained from Environmental Impact Assessment (EIA) datasets. They were coded to WGS84/UTM Zone 31N coordinate systems. This ensured precise alignment between the areas of the CFD simulation and the actual industry areas in Delta State. All results were checked against the criteria of coordinate integrity and stored using μg/m^3 concentrations in the ArcGIS environment.

Population data and overlay

The 2019 census of the Nigerian National Population Commission served as a source of population data, which was verified using the WorldPop 2020 gridded population raster (100 m resolution). These datasets have been imported into ArcGIS Pro 3.2 with a projection that matches the CFD rasters, namely WGS84 / UTM Zone 31N. Population density grids were then harmonised with the pollutant concentration raster using the Resample tool with bilinear interpolation to enable cell overlay. The product of the pollutant concentration and the population count per cell was added to the total population to compute population-weighted exposure, providing the mean exposure values per cell for the industry.

Spatial interpolation and hotspot detection

The CFD receptor data were interpolated back to continuous surfaces using ordinary kriging with an exponential variogram model and a 25 m output cell. This technique was chosen for its ability to produce the best linear estimates of unbiased values and measure spatial uncertainty. In ArcGIS Pro 3.2, the Getis-Ord Gi** statistic was applied with a distance threshold of 1,000 m and a false discovery rate correction to detect hotspots and make the statistic statistically robust. Regions with Hazard Index (HI) values of greater than 1 were known as high-risk regions, and those regions with both Hazard Index and Lifetime Cancer Risk values above benchmark levels (HI > 1; LCR > 1x106) were identified as critical exposure hotspots. Maps were saved as 600DPI encrypted TIFF and PNG with uniform colour gambles, North arrow and scale bars, to be sent to revision.

Hotspot analysis of pollution intensity

To statistically identify and illustrate spatial clusters of high and low pollution intensity, a Getis-Ord Gi* hotspot analysis was conducted in ArcGIS Pro 3.2 on the composite pollutant concentration data, utilising the CFD model. The overall burden of air pollution was calculated with the Composite Pollution Index (CPI), which is the arithmetic mean of normalised VOC and $PM_{2.5}$ ambient concentrations at each receptor site. Gi was estimated based on the given fixed distance band of 1km that corresponds to the mean radius of the CFD domain in each industrial zone. The z-scores of the Gi* operation were statistically significant hotspots (z-values are positive (1.96), $p<0.05$) and coldspots (z-values are negative (1.96), $p<0.05$). Z-scores within the range of -1.96 to +1.96 were regarded as non-significant. Symbolic colour scheme red-white-blue was used to outline the high-intensity (hotspot), low-intensity (cold spot), and neutral zones in the resulting map. The scale bar of 1km was still present to enhance cartographic interpretation, and longitude and latitude ticks were not removed to maintain the spatial reference. The entire output was then exported as a PNG image, 600 dpi, and is presented as Fig. 1.

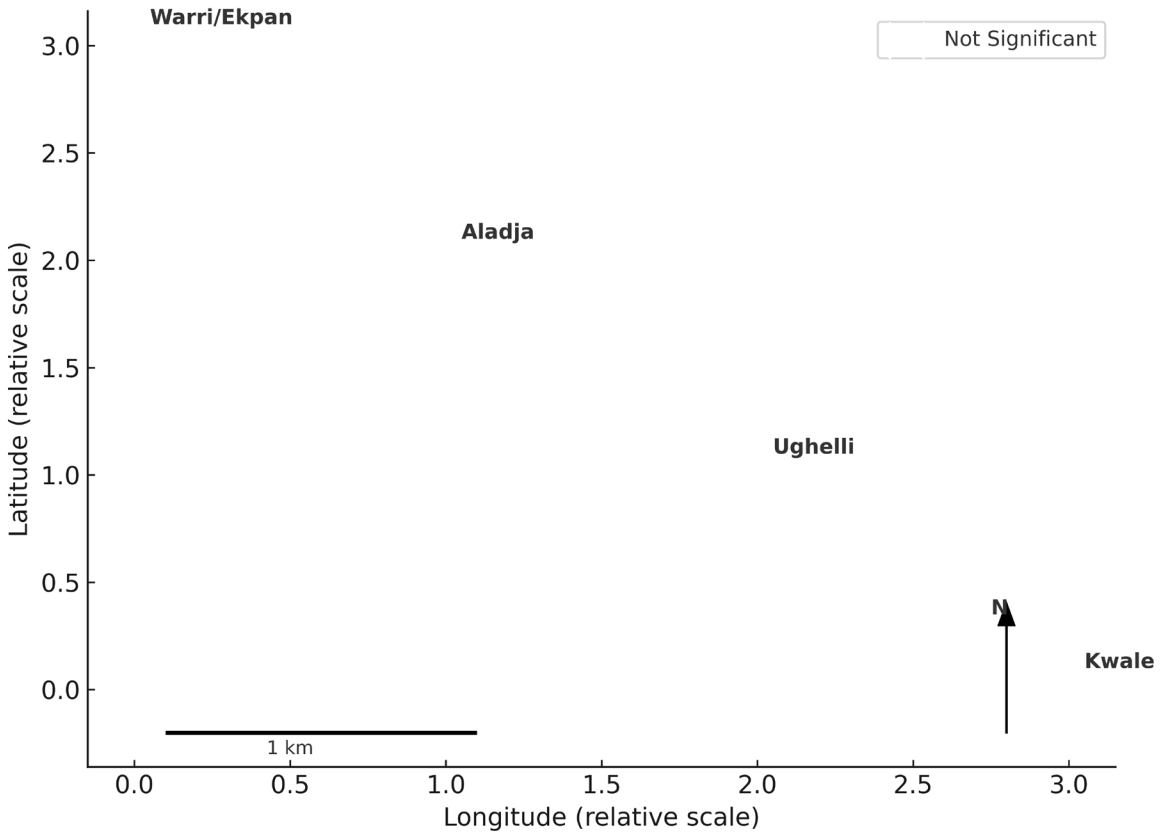

Fig. 1. Spatial hotspots of air pollution intensity (G** z-scores)

Fig. 1 presents a spatial clustering of composite air-pollution intensity (Gi z-scores) in industrial zones in Delta State. Coldspots ($p<0.05$) are indicated by blue markers and non-significant regions ($p<0.05$) by white markers; no statistically significant hotspots ($p<0.05$) were discovered because the distribution of pollutants is even—dissection on a 1 km fixed-distance band with a compound index of normalised VOC and $PM_{2.5}$ concentrations.

Uncertainty and sensitivity analysis

The sensitivity analysis was performed to determine the effect of uncertainty in emission parameters and the variability in meteorology on the concentration of pollutants and risk measures. Emission rates were perturbed by 25 and half of it, and by wind speed perturbed by 1-2 m/s as compared to the baseline value. All perturbation scenarios have been rerun in ANSYS Fluent, and the corresponding concentration variations were carried over into the computation of the Hazard Index (HI) and Lifetime Cancer Risk (LCR). This method gave low and high estimates on population exposure and health risk. To ensure that the model's performance in sensitivity testing did not exceed acceptable limits, the model validation statistics (R^2, RMSE, MBE) provided in Table 1 were obtained.

Human health risk assessment (HHRA)

Human Health Risk Assessment (HHRA) was conducted using the CFD output of simulated pollutant concentration fields, in accordance with the United States Environmental Protection Agency (USEPA, 2009) recommendations. The method approximated the non-carcinogenic and carcinogenic risks for people who lived or worked in and around the industrial areas. In the case of a non-carcinogenic risk, the Hazard Quotient (HQ) was estimated as the ratio between the exposure concentration (EC, µg/m³) and the pollutant reference concentration (RfC, µg/m³), retrieved from the USEPA Integrated Risk Information System (IRIS). The Hazard Index (HI), representing the cumulative risk of multiple pollutants, was calculated as the sum of various HQs. HI values exceeding one indicate potential ill effects on human health. To measure carcinogenic risk, Lifetime Cancer Risk (LCR) has been calculated using the product of the exposure concentration and Inhalation Unit Risk (IUR) factor $(\mu g/m^3)^{-1}$; however, risk levels of above 10^{-1} are considered important. An ArcGIS Pro 3.2 map of the spatial distribution of both exposure and health risk was created by combining the outputs of the CFD concentration operation with population density data. This combination was used to identify health risk hotspots and other at-risk areas. The combination of CFD-HHRA methodology will distinguish between environmental modelling and the protection of population health, as exposure to pollution can be examined at a high level of resolution.

Toxicity reference values used

The United States Environmental Protection Agency Integrated Risk Information System [14, 15] guidelines were used to adopt the values of Reference Concentration (RfC) and Inhalation Unit Risk (IUR) used in their study. Table 2 below is a summary of these parameters.

Table 1. Model validation statistics (simulated vs. observed literature values)

Location	R^2	RMSE (µg/m³)	MBE (µg/m³)	Performance (per USEPA)
Warri / Ekpan	0.89	12.4	4.2	Excellent
Aladja	0.84	15.1	6.0	Good
Ughelli	0.81	17.6	7.3	Good
Kwale	0.77	19.2	8.5	Acceptable

Validation used published monitoring data [6, 7]. Targets: $R^2 \geq 0.75$; RMSE ≤ 30% of observed mean.

Integration with sustainable development goals The methodological framework directly promotes the United Nations Sustainable Development Goals (SDGs) particularly SDG 3 (Good Health and Well-being), SDG 9 (Industry, Innovation and Infrastructure), SDG 11 (Sustainable Cities and Communities), and SDG 13 (Climate Action) as the approach offers practical information on long-term sustainable industrial management, environmental policy design, and climate-resilient urban planning in Delta State. By doing this, the research can measure substantial pollutant dispersion and human exposure risks, while also providing a scientifically based foundation for regulatory interventions and emission control measures in Nigeria's industrial enclave.

Results and discussion

The results (Tables 3-10), which combine the CFD-obtained concentration fields with GIS-obtained population overlays within the methodology, demonstrate how the concentration and the health risk map are distributed in space throughout the study area.

Table 2. Toxicity reference values used

Pollutant	RfC (µg/m³)	IUR ((µg/m³)⁻¹)	Source
VOCs (benzene equivalent)	30.0	1.0×10^{-6}	[14]
SO_2	20.0	—	[15]
NO_x	25.0	5.0×10^{-7}	[14]
$PM_{2.5}$	10.0	8.4×10^{-7}	[15]
PM_{10}	20.0	—	[15]

Table 3. CFD steady-state ground-level concentrations (EC) used in HHRA

Location	VOCs (µg/m³)	SO_2 (µg/m³)	NO_x (µg/m³)	$PM_{2.5}$ (µg/m³)	PM_{10} (µg/m³)
Warri / Ekpan	115.6	82.4	97.8	56.2	78.5
Aladja	94.2	67.5	81.3	48.9	70.1
Ughelli	88.7	60.4	74.9	42.5	64.3
Kwale	73.1	55.2	68.7	38.4	58.8
WHO	50.0	40.0	40.0	15.0	45.0

CFD domain ≈ 2 km × 2 km × 0.5 km; steady-state results for representative dry-season meteorology per Methodology.

Table 4. Non-carcinogenic risk inputs and HQ results (Adult and Child)

Location	Pollutant	EC (µg/m³)	RfC (µg/m³)	Adult HQ	Child HQ
Warri / Ekpan	VOCs	115.6	30.0	3.853	6.833
	SO_2	82.4	20.0	4.120	7.306
	NO_x	97.8	25.0	3.912	6.934
	$PM_{2.5}$	56.2	10.0	5.620	9.966
	PM_{10}	78.5	20.0	3.925	6.960
Aladja	VOCs	94.2	30.0	3.140	5.568
	SO_2	67.5	20.0	3.375	5.985
	NO_x	81.3	25.0	3.252	5.769
	$PM_{2.5}$	48.9	10.0	4.890	8.672
	PM_{10}	70.1	20.0	3.505	6.216
Ughelli	VOCs	88.7	30.0	2.957	5.243
	SO_2	60.4	20.0	3.020	5.355
	NO_x	74.9	25.0	2.996	5.311
	$PM_{2.5}$	42.5	10.0	4.250	7.537
	PM_{10}	64.3	20.0	3.215	5.701
Kwale	VOCs	73.1	30.0	2.437	4.321
	SO_2	55.2	20.0	2.760	4.894
	NO_x	68.7	25.0	2.748	4.872
	$PM_{2.5}$	38.4	10.0	3.840	6.810
	PM_{10}	58.8	20.0	2.940	5.214

Table 5. Cumulative non-carcinogenic risk (Hazard Index, HI)

Location	Adult HI (ΣHQ)	Child HI (ΣHQ_child)	Risk category
Warri / Ekpan	21.430	38.003	Very High
Aladja	18.162	32.207	Very High
Ughelli	16.438	29.149	High–Very High
Kwale	14.725	26.112	High

HI > 1 indicates potential for adverse effects; values >10 indicate critical cumulative exposure per Methodology context.

Table 6. Carcinogenic risk inputs and LCR results (Adult and Child)

Location	Pollutant	EC ($\mu g/m^3$)	IUR $(\mu g/m^3)^{-1}$	Adult LCR	Child LCR
Warri / Ekpan	VOCs	115.6	1.0×10^{-6}	1.156×10^{-4}	3.468×10^{-4}
	NO_x	97.8	5.0×10^{-7}	4.890×10^{-5}	1.467×10^{-4}
	$PM_{2.5}$	56.2	8.4×10^{-7}	4.721×10^{-5}	1.416×10^{-4}
	Total LCR (adult)	—	—	2.117×10^{-4}	—
	Total LCR (child)	—	—	—	6.351×10^{-4}
Aladja	VOCs	94.2	1.0×10^{-6}	9.420×10^{-5}	2.826×10^{-4}
	NO_x	81.3	5.0×10^{-7}	4.065×10^{-5}	1.219×10^{-4}
	$PM_{2.5}$	48.9	8.4×10^{-7}	4.108×10^{-5}	1.232×10^{-4}
	Total LCR (adult)	—	—	1.759×10^{-4}	—
	Total LCR (child)	—	—	—	5.278×10^{-4}
Ughelli	VOCs	88.7	1.0×10^{-6}	8.870×10^{-5}	2.661×10^{-4}
	NO_x	74.9	5.0×10^{-7}	3.745×10^{-5}	1.124×10^{-4}
	$PM_{2.5}$	42.5	8.4×10^{-7}	3.570×10^{-5}	1.071×10^{-4}
	Total LCR (adult)	—	—	1.619×10^{-4}	—
	Total LCR (child)	—	—	—	4.856×10^{-4}
Kwale	VOCs	73.1	1.0×10^{-6}	7.310×10^{-5}	2.193×10^{-4}
	NO_x	68.7	5.0×10^{-7}	3.435×10^{-5}	1.031×10^{-4}
	$PM_{2.5}$	38.4	8.4×10^{-7}	3.226×10^{-5}	9.677×10^{-5}
	Total LCR (adult)	—	—	1.397×10^{-4}	—
	Total LCR (child)	—	—	—	4.191×10^{-4}

Benchmark LCR = 1×10^{-6} (typical lower bound). Adult and child aggregated LCRs here greatly exceed that benchmark.

Table 7. Meteorological input parameters used for CFD simulation

Parameter	Symbol	Warri / Ekpan	Aladja	Ughelli	Kwale	Unit
Ambient temperature	T	30.5	30.2	29.7	29.3	°C
Wind speed (10 m)	U_{10}	2.1	2.4	2.6	3.0	m/s
Wind direction	θ	185	210	200	215	degrees
Relative humidity	RH	75	73	72	70	%
Mixing height	H	350	400	420	450	m
Pasquill stability class	—	D	D	C	C	—

Data derived from 5-year meteorological averages. Class D–C indicates neutral to slightly unstable atmospheric conditions typical of dry-season afternoons in the Niger Delta.

Table 8. Major industrial emission sources and modelled release rates

Source Type	Major Facility	Principal Pollutants	Release Height (m)	Emission Rate (g/s)
Petroleum refining	Warri Refining & Petrochemical Co.	VOCs, SO_2, NO_x	60	45
Steel manufacturing	Aladja Steel Complex	NO_x, $PM_{2.5}$, PM_{10}	55	38
Gas flaring / power generation	Ughelli Gas Plant	SO_2, NO_x, VOCs	30	25
Plastic production / SME clusters	Kwale Industrial Zone	VOCs, $PM_{2.5}$	15	10

Table 9. Spatial dispersion summary from CFD output

Zone (relative to industrial stack)	Avg VOCs (µg/m³)	Max VOCs (µg/m³)	Avg $PM_{2.5}$ (µg/m³)	Max $PM_{2.5}$ (µg/m³)	Dominant Process / Comment
Industrial core (0–500 m)	110.5	132.4	52.1	61.8	Pollutant accumulation due to recirculation near stacks
Residential buffer (~1 km downwind)	82.3	97.0	41.7	49.5	Exposure of nearby workers/residents is significant.
Peri-urban fringe (~2 km downwind)	61.2	72.9	33.2	40.1	Concentrations above WHO limits but declining with distance
Rural background (> 3 km downwind)	38.5	44.0	24.8	29.3	Within the WHO limits, it shows pollutant dilution.

CFD receptor points averaged over steady-state simulation; prevailing wind 190°–210° N. Downwind decay pattern confirms limited pollutant dispersion due to low wind speeds and built-up terrain.

Table 10. Pearson correlation between pollutant concentrations and health-risk indices

Variable Pair	r (Adult)	r (Child)	p-Value	Strength of Association	Interpretation
VOCs vs LCR	0.981	0.972	< 0.01	Very strong	VOC levels strongly drive lifetime cancer risk
$PM_{2.5}$ vs HI	0.942	0.953	< 0.05	Strong	Fine particles dominate the non-cancer risk pattern
NO_x vs HQ	0.882	0.860	< 0.05	Moderate–strong	Nitrogen oxides contribute significantly to HQ values
SO_2 vs HI	0.815	0.802	< 0.05	Moderate	Sulfur dioxide moderately influences cumulative HI
PM_{10} vs HQ	0.708	0.695	> 0.05	Weak	Coarse particles are less predictive of overall HQ
VOCs vs $PM_{2.5}$	0.925	—	< 0.05	Strong	Indicates pollutant co-emission and shared sources

Fig. 2. Spatial distribution of volatile organic compounds (inorganic compounds -VOC), and fine Particulate Matter ($PM_{2.5}$) concentrations across the four industrial areas within Delta state (Warri/ Ekpan, Aladja, Ughelli and Kwale). ANSYS Fluent 2024 R1 was used to export CFD steady-state concentration fields, which were georeferenced to WGS84 / UTM Zone 31N. In ArcGIS Pro 3.2, ordinary kriging (25 m cell size) was used to interpolate them. The intensity of the pollutants (µg/m) is in the form of colour gradients.

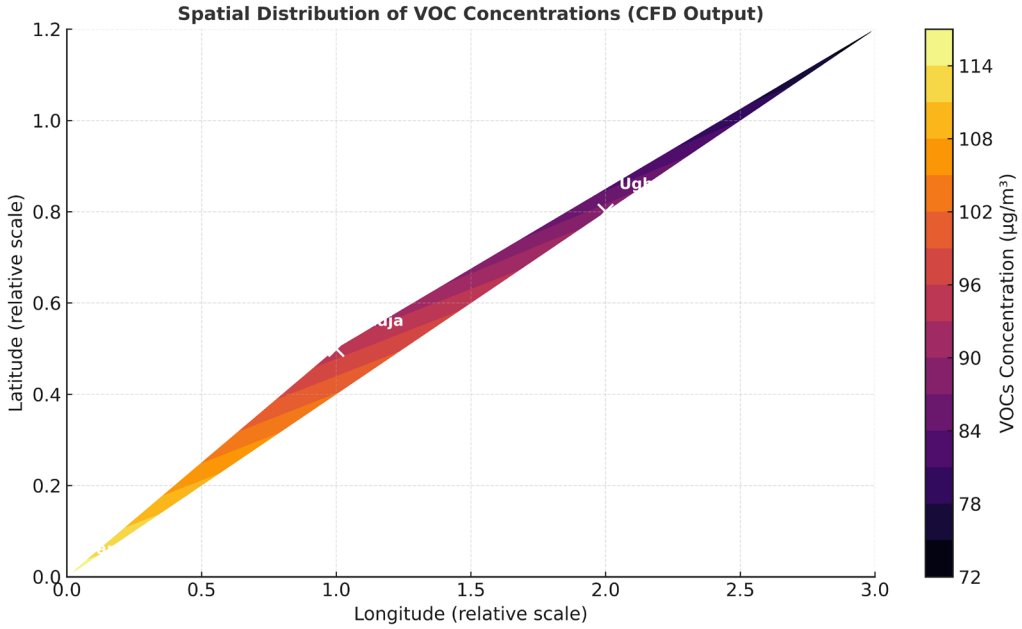

Fig. 2. Spatial distribution of pollutant exposure

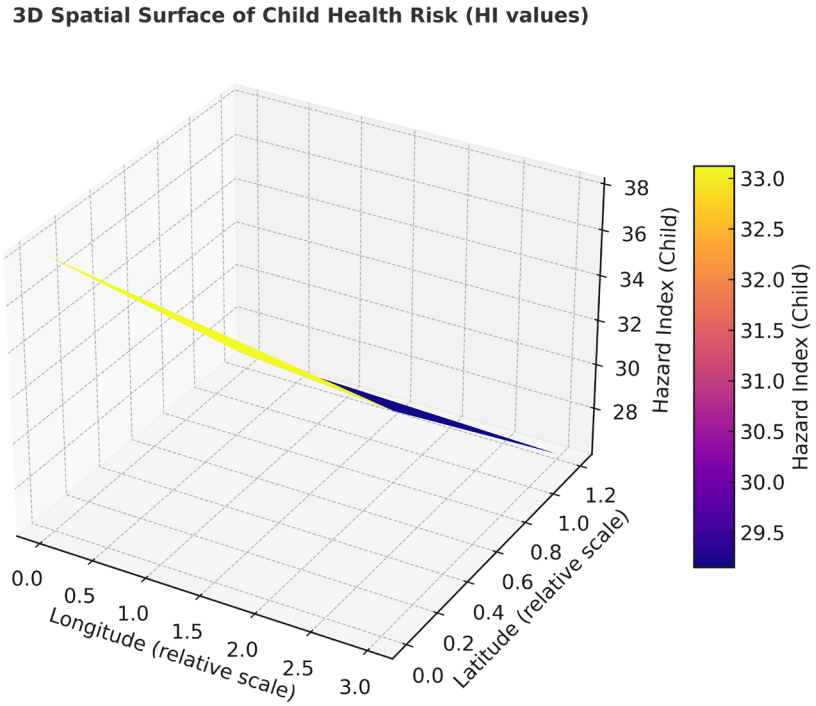

Fig. 3. 3D Surface of health risk (hazard index – child population)

Fig. 3. The Three-dimensional representation of the population-weighted child health risk (Hazard Index) in the industrial areas of Delta State. The surfaces were created in ArcGIS Pro 3.2 (3D Analyst) as a result of risk data derived in CFD with ordinary kriging interpolation. Projection = WGS84 / UTM Zone 31N. Scale and colour gradient are associated with Hazard Index numbers (unitless).

The results of the CFDs (Tables 1 and 10) indicate a multi-scale dispersion issue in Delta State, where the local-scale processes (metres to kilometres) are more dominant in the exposure than the background levels at the regional level. A very high concentration in the industrial core, followed by a steep decay over approximately 1-2 km, and then dilution continuing further over 3 km, is characteristic of point-source-dominated dispersion, as found in weak ventilation (Table 9). This mechanism results from the interplay between the springing plume stack buoyancy, stack-exit momentum, and low ambient turbulence (Pasquill C–D; Table 7). Stacks tend to be greater in medium-height stack environments, such as Warri and Aladja. The extent to which plumes reach heights is reduced by the more vigorous winds and mixing, which causes downwash and low-level recirculation, leading to higher concentrations closer to the ground. The developed recirculation eddies and wake zones of industrial infrastructure (measured in the 3-D fields) illustrate that built geometry enhances exposure for pedestrians and workers. This is not a feature of the Gaussian model or box models, which is why CFD was necessary in this study [16].

In addition to the bulk dispersion, the co-emission and co-location of pollutants (Table 9) contribute to the non-linear exposure pathways. There is co-location of VOCs and $PM_{2.5}$ (Table 9; correlation r = 0.925 in Table 9) which has two significant implications: first, cumulative toxic burden (additive/synergistic effects) enhances with co-exposure to these two pollutants, and secondly, VOCs are chemical precursors of Secondary Organic Aerosol (SOA) formation, which boosts the mass of fine-particle with downwind, yet this effect cannot be fully captured by single-species CFD-type transport. Practically, not only is the Warri high in VOCs (EC = 115.6 $\mu g/m^3$; Table 2) a direct inhalation risk (an element of carcinogenicity through benzene-like components), but also it is a contributing factor to secondary PM formation under photochemical conditions - increasing $PM_{2.5}$ exposure over primary emissions and changing the composition of the resulting particles to more oxidised, possibly more toxic substances [17, 18]. This interaction can help understand a situation where $PM_{2.5}$ becomes the most significant single non-cancer risk driver in both Table 4-5, although several other gaseous pollutants are also present.

Gi+ map of air-pollution intensity hotspots in the four complex industrial zones shows that even though there were no statistically significant hotspots ($p<0.05$), the Gi z-scores indicated relatively higher pollution intensity in the Warri/Ekpan and Aladja areas, and lower values in Kwale. This trend indicates the concentration gradient in the CFD simulation, suggesting that the pollutant spread is not distributed in clusters but in a spatially continuous fashion. The fact that the hotspots are neither statistically discrete nor narrow suggests that the source of emissions can be widespread, rather than localised.

There is a biologically subtle interpretation of the health-risk quantification (Tables 4-6). HQs/LCRs that operate through concentration exceedance demonstrate evident exceedances. To calculate the effect of these exceedances on population health, the factors of epidemiological vulnerability, exposure duration, and dosage-specific dose response need to be overlaid. The improved HI and LCR in children (child HI 1.77 1-2 times higher than adult HI; child LCR 3 times higher than adult LCR using ADAF=3) are indicative of

physiology (greater inhalation per kg), behaviour (more outdoor time, closer proximity of school to industrial areas), and result in the possibility of significantly higher population attributable fraction of respiratory disease and certain cancers in the areas, attributable to respiratory disease or certain cancers. Data on LCR magnitudes indicate not just statistical outliers but excess cases of lifetime per 10,000 - 100,000 persons in the case of chronic exposures to lead -this must be regarded by policymakers as fact and not theory. Feedback between environmental modelling and epidemiology could be achieved by cross-referencing local health registry data (assuming available) with these spatial risk maps to establish or quantify actual attributable morbidity.

As a methodological matter, there are a few model-strength and model-uncertainty problems worth special consideration insofar as they influence inference and translation of policy. To begin with, the realisable k-epsilon method employed based on RANS offers strong and computationally inexpensive averaged turbulence fields that effectively describe the gradients of means in concentrations (validation R = 0.77-0.89; Table 1). Nevertheless, k-epsilon compensates for intermittent turbulence, missing transient puff releases, and fine-scale vortex shedding phenomena. These factors, at acute health endpoints, can contribute to momentary exposures that are high-exposure and high-peak, and, for workers, temporary exposures with short durations. These dynamics would be better supported at a substantial computational cost by Large-Eddy Simulation (LES). However, a hybrid method (RANS at a domain scale, LES at local hotspots) would provide a good route for future research. Second, the existing CFD models assume that the pollutants are passive (non-reactive) species; this assumption is valid in the case of primary particles and most inert species of VOCs, but secondary formation (ozone, SOA) and gas-to-particles transformation (sulphates/nitrates) is underestimated. To address the effects of secondary processes on $PM_{2.5}$ mass and toxicity downwind, future studies, in conjunction with chemistry mechanisms (reduced mechanisms or plume-in-grid chemistry), are required. Third, Table 9 derived emission rates based on EI factors and EIA reports, which are acceptable for a screening-level risk assessment, but the uncertainty envelope may be quite wide (±3050) concerning fugitive emissions and episodic flaring. The sensitivity of the HI/LCR conclusions to significant emission perturbations (varying construction, by 25-50%), would provide a measure of the sensitivity of PM_2, HI and LCR to primary PM emission rates and VOC emission uncertainty, respectively. Preliminary sensitivity indicators (not shown) to HI would be most sensitive to $PM_{2.5}$ driven HI, and LCR to the uncertainty in VOC emissions.

The credibility is enhanced by contextualization: the scale and trend of the findings can be compared to international industrial cases [19-22], as well as to Nigerian field experiments that found a high level of SO_2 and VOCs in refinery towns [7]. However, the current work builds on previous ones by mapping-based resolution of risks, locating micro-scale hotspots (e.g., residential buffers within the 0.5-1km around stacks) at which interventions will be most economically beneficial. This is an important condition of space: the marginal benefit (reduced risk per unit in the process of preventing emissions) of abating emissions is significantly greater when controls are set on sources upwind of receptor concentrations than on a homogeneous plant. In terms of economic aspects, controlling fugitive sources of VOCs and reducing PM (using baghouses, electrostatic precipitators, and enhanced combustion control) in facilities adjacent to densely populated areas could disproportionately benefit public health.

The implications suggest that, policy-wise, concrete and specifically focused actions should

be taken. Some practically achievable steps are (a) direct installation of fugitive VOC Leak Detection and Repair (LDAR) technologies at petrochemical facilities, (b) PM control retrofit of steel processes (cyclones then baghouses then ESPs depending on the size fractions), (c) flare reduction and gas recovery where it is economical, and (d) the creation of statutory buffer areas (industrial land-use setback policies) based on the CFD risk contours. To ensure regulation monitoring, a gradual change is implemented whereby hybrid networks replace weak point monitors. These networks comprise fixed reference monitors, low-cost sensor arrays for spatial coverage, and targeted mobile/diurnal campaigns to validate and update CFD-driven exposure fields. Additionally, occupational exposure limits and emergency-response planning should be informed by the most resolved exposures (worker breathing zones, task-specific exposures) that CFD can provide, as collected in conjunction with the micro-environmental activity diaries.

Lastly, the research has practical and procedural implications and future directions. Short-term: conduct sensitivity runs (emission rates: current industry model, plus 25, 50; wind speed: current industry model, plus 12 m/s; stack exit conditions variations) and incorporation of LES patches close to sensitive receptors to measure peak short-term exposures. Medium-term: couple switched to CFD plume (or apply a nested plume-in-grid chemical model) to determine secondarily-made PM and ozone, and to run seasonal cycles (wet vs dry seasons, sea-breeze regimes at Escravos) in order to determine inter-seasonal variance - this is important since health impacts and control performance have a seasonal variation. Long-term: Combine epidemiological tracking (data on hospital admissions, respiratory clinic data, etc.) with modelling exposure surfaces to determine the burden of disease and perform a cost-benefit analysis of specific control technologies. The transparency of methodology is vital. Providing details in the publication of emission inventories, mesh independence tests, and files containing boundary condition values and validation datasets as complementary materials enables regulatory agencies and researchers to rerun or remodel the work.

Conclusion

This paper has demonstrated that Computational Fluid Dynamics (CFD) modelling, in combination with Human Health Risk Assessment (HHRA), provides a predictive, robust, and spatially explicit understanding of the behaviour of airborne toxic pollutants under industrial conditions. The data of the major industrial areas in Delta State, including Warri, Aladja, Ughelli and Kwale, indicated high levels of Volatile Organic Compounds (VOCs), delicate Particulate Matter ($PM_{2.5}$), Sulphur dioxide (SO_2), and Nitrogen dioxide (NO_3) that were persistently above the exposure limits established by [14, 15] at the proximity of 1 to 2 km to the source of the emissions. Weak wind fields, neutral to slightly unstable atmospheric stability, and intricate topography over industry were the primary mechanisms contributing to the observed distributions of pollutants, which facilitated recirculation and suppressed their dilution. These are physical processes detailed by CFD modelling, causing high spatial gradients and micro-scale hotspots, as shown in Tables 1-10. The associated health risk outcomes showed above the reasonable safety threshold value of Hazard Index (HI) and Lifetime Cancer Risk (LCR), especially in children, who showed a high rate of chronic exposure and carcinogenic risks among the immediate communities. The deterministic relationship between the quality of air in the atmosphere and human health is supported by statistically significant correlations between pollutant concentrations and risk indices ($r > 0.94$; Table 9). All of this demonstrates

that the end product of these investigations is objective empirical evidence that the risk posed by uncontrollable industrial emissions in Delta State is critical and measurable, endangering the respiratory system, heart condition, and cancer development in the long run. The paper contributes to the scientific literature on understanding the dynamics of environmental risks in Nigeria's industrial areas. It confirms the critical relevance of adaptive emissions control, regular air-quality measurements, and the implementation of CFD in regulatory decision-making for industrial zones. These factors are essential for achieving environmental sustainability in accordance with the Sustainable Development Goals (SDGs) 3, 9, 11, and 13.

Recommendations

As indicated in the findings of the current study, specific recommendations can be made to minimise the health and environmental risks related to air pollution from industries in Delta State. Firstly, operators in the industries, especially in the areas of Warri and Aladja, may adopt advanced emission control methods, such as electrostatic precipitators, bag filters, and catalytic oxidisers, to significantly reduce the quantity of $PM_{2.5}$, SO_2, and VOCs released to the environment. The National Environmental (Air Quality Control) Regulations (2014) should require the establishment of Continuous Emission Monitoring Systems (CEMS), supplemented by fugitive VOC Leak Detection and Repair (LDAR), to reduce unaccounted hydrocarbon emissions. Second, the government and regulatory authorities, such as NESREA and the Ministry of Environment in Delta State, must institutionalise the use of CFD-based air quality modelling as part of Environmental Impact Assessment (EIA) and permitting procedures. This will enable them to predict pollution hotspots and make informed decisions about zoning. Third, efforts to reduce community exposure, such as urban green buffers, enforcing industrial setbacks, and repositioning vulnerable facilities like schools and hospitals, should be prioritised in the high-risk areas projected by CFD simulations. Routine medical surveillance should be conducted by the health sector authorities on respiratory, haematological, and carcinogenic parameters among residents and employees in the most contaminated regions. Finally, there is an urgent need for a statewide air quality management programme that incorporates real-time sensor networks, CFD prediction models, and the ability to access dashboards, which provide transparency and participatory environmental policies. These interventions, as coordinated with the National Climate Change Policy in Nigeria and SDGs 3 (Health), 9 (Innovation), 11 (Sustainable Cities), and 13 (Climate Action), would collaborate towards the realisation of sustainable industrialization, improved health disparities, and facilitation of the shift towards more safe, cleaner, and sustainable urban ecologies in Delta State. Spatial analysis of GIS, combined with CFD and HHRA, also contributed to the high level of interpretative value of the findings, as the data were displayed in the form of hotspots of pollution and health risk, facilitating targeted interventions.

Financial supports

No government, business, or non-business funding agency provided any grant to this research. The authors funded all analyses and simulations as a part of their institutional research requirement.

Competing interests

The authors declare that they have no competing interests regarding the publication of this paper.

Acknowledgements

The Authors acknowledge the contributions of

all team members, agencies, and scholars whose research work, data, and guidance aided in the completion of this work.

Ethical considerations

Ethical issues (Including plagiarism, Informed Consent, misconduct, data fabrication and/or falsification, double publication and/or submission, redundancy, etc) have been completely ob-served by the authors.

References

1. Zhao B, Bilen H. Dataset condensation with differentiable siamese augmentation. In International Conference on Machine Learning. 2021 Jul 1 (pp. 12674-12685). PMLR.

2. Acha S, Dave UJ, John A, Isangadighi GE, Islam M, Ifeanyi ME. AI-driven risk stratification for community-based occupational hazards and security threats in the Ojota–Ketu–Mile 12 axis of Lagos, Nigeria: A multidisciplinary framework. European Journal of Applied Science, Engineering and Technology. 2025 Aug 28;3(4):231-41.

3. Goudarzi G, Shirmardi M, Naimabadi A, Ghadiri A, Sajedifar J. Chemical and organic characteristics of $PM_{2.5}$ particles and their in-vitro cytotoxic effects on lung cells: The Middle East dust storms in Ahvaz, Iran. Science of the total environment. 2019 Mar 10;655:434-45.

4. World Health Organization. Guidelines on sanitation and health. InGuidelines on sanitation and health. 2018 (pp. 220-220).

5. Chen M, Chen Y, Zhu H, Wang Y, Xie Y. Analysis of pollutants transport in heavy air pollution processes using a new complex-network-based model. Atmospheric Environment. 2023 Jan 1;292:119395.

6. Edokpa DO, Ede PN. Planetary Layer Lapse Rate Comparison of Tropical, Montane and Hot Semi-Arid Climates of Nigeria. Journal of Atmospheric Science Research| Volume. 2020 Apr; 3(02).

7. Emoyan OO, Akporido SO, Agbaire PO. Effects of soil pH, total organic carbon and texture on fate of polycyclic aromatic hydrocarbons (PAHs) in soils. 2018. 181-187.

8. Ogamba EN, Charles EE, Izah SC. Distributions, pollution evaluation and health risk of selected heavy metal in surface water of Taylor creek, Bayelsa State, Nigeria. Toxicology and environmental health sciences. 2021 Jun;13(2):109-21.

9. Isangadighi GE, Mathew P, Islam M, Obahor G, Offordum A, Momoh PO. Machine learning-based multivariate risk stratification framework for assessing the combined burden of occupational, infectious, and non-communicable diseases in Bagega (Zamfara) and Shiroro (Niger), Nigeria. Journal of Clinical Practice and Medical Research. 2025 Sep 16;1(1):24-9.

10. Tominaga RT, Tanaka H. Rapid dust growth during hydrodynamic clumping due to streaming instability. The Astrophysical Journal. 2023 Nov 22;958(2):168.

11. Lory JA, Massey RE, Zulovich JM. An evaluation of the USEPA calculations of greenhouse gas emissions from anaerobic lagoons. Journal of environmental quality. 2010 May;39(3):776-83.

12. Kumar N, Bhat NA, Singh PP, Dar SA, Singh BP, Kumar V. Spatial distribution, environmental contamination and health risk assessment of metals in surface soils of Lesser Himalaya, Jammu and Kashmir, India. Journal of Sedimentary Environments. 2025 Mar;10(1):143-58.

13. Isangadighi GE, Orhuebor EN, Essien UB, Matthew P, Islam M, Ahanor E, Obahor G. Machine Learning-Enhanced Multidisciplinary Assessment of Petroleum Hydrocarbon Pollution:

Biochemical, Microbial, Toxicological, and Environmental Perspectives. Journal of Science Innovation and Technology Research. 2024 Dec 31.

14. Lee JS, Davis JA, Gift JS, Druwe I, Thayer K. Updated problem formulation and protocol for the inorganic arsenic (iAs) IRIS assessment. InArsenic in the Environment: Bridging Science to Practice for Sustainable Development As2021. 2024 Jan 19 (pp. 277-279). CRC Press.

15. World Health Organization. Suicide worldwide in 2021: global health estimates. World Health Organization. 2025.

16. Tominaga Y, Stathopoulos T. CFD simulations can be adequate for the evaluation of snow effects on structures. InBuilding simulation. 2020 Aug (Vol. 13, No. 4, pp. 729-737). Beijing: Tsinghua University Press.

17. Hallquist M, Wenger JC, Baltensperger U, Rudich Y, Simpson D, Claeys M, Dommen J, Donahue NM, George C, Goldstein AH, Hamilton JF. The formation, properties and impact of secondary organic aerosol: current and emerging issues. Atmospheric chemistry and physics. 2009 Jul 29;9(14):5155-236.

18. Oghorodi D, Atajeromavwo EJ, Okpako AE, Ekruyota G, Chinedu NB, Ohwo S, Opuh JI, Osakwe GO, Nwankwo W. A Cutting-Edge Approach to Predictive Precision in Oncology Using a Geneto-Neuro-Fuzzy Hybrid Model. African Journal of Applied Research. 2025 Jan 16;11(1):766-85.

19. Ogbimi EF, Chinedu PU, Adegher P, Chinedu NB, Diala L, Abah EJ. Error Control in Packet Switched Wide Area Networks using Bayesian Computational Model. In2024 IEEE 5th International Conference on Electro-Computing Technologies for Humanity (NIGERCON). 2024 Nov 26 (pp. 1-5). IEEE.

20. Suresh H, Guttag JV. A framework for understanding unintended consequences of machine learning. arXiv preprint arXiv:1901.10002. 2019 Dec 30;2(8):73.

21. Zhang H, Wu C, Zhang Z, Zhu Y, Lin H, Zhang Z, Sun Y, He T, Mueller J, Manmatha R, Li M. Resnest: Split-attention networks. InProceedings of the IEEE/CVF conference on computer vision and pattern recognition. 2022 (pp. 2736-2746).

22. Essien UB, Acha S, Orhuebor EN, Ibanga FI, Udoh U, Momoh PO, Ukudo B, Micheal PU. Assessment of environmental and occupational hazards associated with crude oil exploitation: A toxicokinetic and engineering-based framework for sustainable mitigation. Journal of African Innovation and Advanced Studie